

# Bloch oscillations in an aperiodic one-dimensional potential

F. A. B. F. de Moura,<sup>1</sup> M. L. Lyra,<sup>1</sup> F. Domínguez-Adame,<sup>2</sup> and V. A. Malyshev<sup>3</sup>

<sup>1</sup>*Departamento de Física, Universidade Federal de Alagoas, Maceió AL 57072-970, Brazil*

<sup>2</sup>*GISC, Departamento de Física de Materiales, Universidad Complutense, E-28040 Madrid, Spain*

<sup>3</sup>*Institute for Theoretical Physics and Materials Science Center,*

*University of Groningen, Nijenborgh 4, 9747 AG Groningen, The Netherlands\**

We study the dynamics of an electron subjected to a static uniform electric field within a one-dimensional tight-binding model with a slowly varying aperiodic potential. The unbiased model is known to support phases of localized and extended one-electron states separated by two mobility edges. We show that the electric field promotes sustained Bloch oscillations of an initial Gaussian wave packet whose amplitude reflects the band width of extended states. The frequency of these oscillations exhibit unique features, such as a sensitivity to the initial wave packet position and a multimode structure for weak fields, originating from the characteristics of the underlying aperiodic potential.

PACS numbers: 78.30.Ly; 71.30.+h; 73.20.Jc; 72.15.Rn

## I. INTRODUCTION

The nature of one-electron eigenstates has a significant influence on the electronic transport properties of solids. In pure periodic systems, the one-electron eigenstates are Bloch waves which are translational invariant and all delocalized in the thermodynamic limit. In the absence of scattering, the system behaves as a perfect conductor whenever the Fermi energy falls into the conduction band. Disorder, originating from lattice imperfections, modifies the nature of the one-electron eigenstates. For a relatively weak disorder (of a magnitude smaller than the band width), the states at the band center may remain extended,<sup>1</sup> but loses the phase coherence at large distances. Those states, which lie near the band edges, turn out to be exponentially localized. Well defined energies, which separate localized and extended states, are known as mobility edges.<sup>2</sup> The metallic or insulating character of the system at zero temperature depends now on whether the Fermi level is located within the phase of delocalized or localized states, respectively. In the former case, the system shows a finite conductivity, while in the latter one it behaves as a perfect insulator. A large compared to the band width disorder localizes all the one-electron eigenstates, and the conductivity of the system vanishes at zero temperature.

The above picture holds for three-dimensional (3D) systems (for an overview see Refs. 3 and 4). In lower dimensions the effect of disorder is much more dramatic. In particular, uncorrelated disorder of any magnitude causes exponential localization of all one-particle eigenstates in one dimension (1D)<sup>5,6</sup> and weak localization in two dimensions (2D).<sup>6</sup> At the end of eighties and beginning of nineties it was realized, however, that extended states may survive in 1D systems when the disorder distribution is correlated.<sup>7,8,9,10,11,12,13,14,15</sup> Thus, a short-range correlated disorder was found to cause the extended states at special resonance energies; they form a set of null measure in the density of states in the thermodynamic limit.<sup>7,8,9,10,11</sup> Because of that mobility edges do not ex-

ist. Oppositely, long-range correlations in the disorder distribution support a finite fraction of the delocalized states<sup>13,14</sup> and give rise to the existence of mobility edges. In Refs. 16,17,18 it was argued that a nonrandom long-range inter-site coupling represents a one more driving force to delocalize one-particle states in 1D<sup>16,17,18</sup> and 2D<sup>18</sup> geometries. The theoretical predictions about suppression of localization in 1D geometry due to correlations in the disorder distribution were recently confirmed experimentally in semiconductor superlattices with intentional correlated disorder<sup>12</sup> as well as in single-mode wave guides with inserted correlated scatterers.<sup>15</sup>

Another class of 1D models, that can exhibit an Anderson-like localization-delocalization transition, involves a nonrandom, deterministic potential which is incommensurate with the underlying lattice. Several models of this type have been extensively investigated in the literature, and the localized or extended nature of their eigenstates has been related to general characteristics of the incommensurate potentials.<sup>19,20,21,22,23</sup> An interesting class among them is represented by aperiodic slowly varying potentials. The latter support the mobility edges in a very close analogy with the standard 3D Anderson model.<sup>22</sup>

Recently, there appeared a renewed interest in the dynamics of an electron in crystals subjected to a uniform static electric field. Under this condition, the electronic wave function displays so-called Bloch oscillations,<sup>24,25,26</sup> the amplitude of which is proportional to the band width. The electronic Bloch oscillation was observed for the first time in semiconductor superlattices<sup>27</sup> (for an overview see Ref. 28). It is to be noticed that in bulk materials, this coherent regime of electron motion is hard to realize because the electron dephasing time due to scattering on defects and phonons is usually shorter than the period of Bloch oscillations. An exception represents semiconductor superlattices, in which the opposite situation takes place. The unit cells in these materials are large enough to make the period of Bloch oscillations shorter than the electron dephasing time, so that several periods of os-

cillations can be detected.<sup>27</sup> A similar phenomenon of sustained oscillations of the electromagnetic field, named photon Bloch oscillations, have also been reported in two-dimensional wave guide arrays and optical superlattices based on porous silicon.<sup>29</sup>

Recently we investigated theoretically Bloch oscillations in a 1D disordered system with diagonal long-range correlated disorder and found that this type of correlations in disorder does not destroy the coherence of Bloch oscillations.<sup>30</sup> The amplitude of the latter was found to carry information about the energy difference between the two mobility edges. This result resembles the one that exists for an ideal Bloch band, where the amplitude of oscillation is proportional to the bandwidth.

In this work, we further contribute to the general understanding of the phenomenon of electronic Bloch oscillations in non-periodic low-dimensional systems exhibiting mobility edges. To this end, we will focus on the biased wave packet dynamics of a single electron moving in a lattice with an aperiodic slowly varying potential. As potential correlations are long-ranged, sustained oscillations may be anticipated, similarly to our previous results.<sup>30</sup> It should be noticed, however, that the deterministic nature of the potential and its aperiodicity introduce new features to the Bloch oscillations. We solve numerically the time-dependent Schrödinger equation and compute the time dependence of the average electron position. Fourier analysis is implicated to reveal regularities of the electron motion.

## II. MODEL SYSTEM AND RELEVANT MAGNITUDES

We consider a tight-binding Hamiltonian on a regular 1D open lattice of spacing  $a$  with an aperiodic slowly varying potential and a uniform static electric field<sup>26,31</sup>

$$\mathcal{H} = \sum_{n=1}^N \left( \tilde{\varepsilon}_n - e\mathcal{F}an \right) |n\rangle\langle n| - J \sum_{n=1}^{N-1} \left( |n\rangle\langle n+1| + |n+1\rangle\langle n| \right), \quad (1)$$

where  $|n\rangle$  is a Wannier state localized at site  $n$  with energy  $\tilde{\varepsilon}_n$ ,  $\mathcal{F}$  is the external uniform electric field and  $-e$  is the charge of the particle. The hopping amplitude is assumed to be uniform over the entire lattice with  $J > 0$ . In terms of the Wannier amplitudes  $\psi_n(t) = \langle n | \Psi(t) \rangle$ , the time-dependent Schrödinger equation reads<sup>26</sup>

$$i\dot{\psi}_n = (\varepsilon_n - Fn)\psi_n - \psi_{n+1} - \psi_{n-1}, \quad (2)$$

where we introduced the dimensionless magnitudes  $\varepsilon_n = \tilde{\varepsilon}_n/J$  and  $F = e\mathcal{F}a/J$ . Time is expressed in units of  $\hbar/J$ .

Here, we will consider an on-site potential  $\varepsilon_n$  given by<sup>22</sup>

$$\varepsilon_n = V \cos(\pi\alpha n^\nu), \quad V > 0, \quad (3)$$

with  $V$ ,  $\alpha$  and  $\nu$  being variable parameters (an example of  $\varepsilon_n$  is depicted in Fig. 1). For  $\nu = 1$  this is just Harper's model, for which a rational  $\alpha$  describes a crystalline solid, whereas an irrational  $\alpha$  results in an incommensurate potential. Dynamical localization in the Harper's model under the action of electric fields was studied in Ref 32. In the following, we restrict our study to an interesting range of parameters  $0 < \nu < 1$  and  $0 < V < 2$ . It was demonstrated for this case that there exists a phase of extended states near the band center, which is separated by the two mobility edges  $\pm E_c = \pm(2 - V)$  from two phases of localized states closer to the band edges.<sup>22</sup>

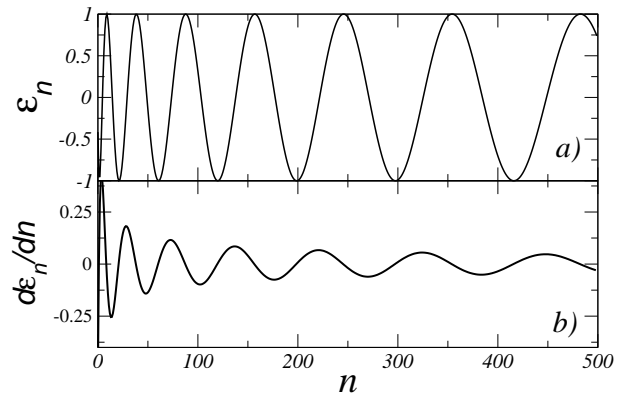


FIG. 1: (a) Aperiodic slowly varying potential calculated for  $V = 1$ ,  $\pi\alpha = 1$ , and  $\nu = 0.5$ ; b) The potential derivative showing the decrease of its local maxima on increasing the site index  $n$ .

The pertinent quantities we will use to characterize the dynamics of the electron wave packet are its mean position (centroid)

$$x(t) = \sum_{n=1}^N (n - n_0) |\psi_n(t)|^2, \quad (4a)$$

and the *spread* of the wave function (square root of the mean squared displacement)

$$\sigma(t) = \left( \sum_{n=1}^N [n - \langle n(t) \rangle]^2 |\psi_n(t)|^2 \right)^{1/2}, \quad (4b)$$

where  $\langle n(t) \rangle = \sum_{n=1}^N n |\psi_n(t)|^2$ . As the initial packet is assumed spatially narrow, one has contributions to the wave packet dynamics, coming from a wide spectrum of eigenstates of the Hamiltonian (1).

In ideal lattices, a uniform field causes the electron wave packet to oscillate in space and time. The amplitude and the period of these oscillations are estimated semiclassically as  $L_c = W/2F$  and  $\tau_B = 2\pi/F$ , respectively (see, e.g., Ref. 33), where  $W$  here is the width of the Bloch band in units of the hopping constant  $J$ . Subsequently, the frequency of the harmonic motion is  $\omega = F$ , for the chosen units. The above picture was shown to

remain valid when long-range correlated disorder is introduced with  $W$  being replaced by the band width  $W_c$  of delocalized states.<sup>30</sup> In what follows, we provide numerical evidences of that the above semiclassical picture still holds for the present aperiodic system, although this requires a renormalization of the applied electric field due to the presence of the on-site aperiodic potential.

### III. NUMERICAL RESULTS

We numerically solved the time-dependent Schrödinger equation (2) by means of an implicit integration algorithm.<sup>34</sup> The initial wave packet was chosen to be a narrow Gaussian of width  $\sigma = 1$ , centered at an arbitrary lattice site  $n_0$ :

$$\psi_n(0) = A(\sigma) \exp \left[ -\frac{(n - n_0)^2}{4\sigma^2} \right], \quad (5)$$

where  $A(\sigma)$  is a normalization constant. To improve stability of the numerical algorithm, we set the electric potential to vanish at the initial site, replacing  $Fn$  by  $F(n - n_0)$  in Eq. (2). This produces only a shift in the origin of energy with no physical effect.

#### A. Unbiased dynamics

We start our analysis of the electron motion by studying the wave packet dynamics in the absence of the external field. The parameters of the aperiodic potential are set hereafter to  $V = 1$ ,  $\pi\alpha = 1$ , and  $\nu = 0.5$ . In Fig. 2(a), we depicted the time evolution of the centroid of a wave packet, which initially was located at site  $n_0 = 48$ . It is worth to notice that the potential slope at this point is negative (see Fig. 1). The inset in Fig. 2(a) demonstrates that at the earlier stage of motion, the centroid oscillates harmonically, but loses the phase memory rapidly. The frequency of these few oscillations is about 0.13 in the dimensionless units. We show below that this number is directly related to the strength of the local field, produced by the aperiodic potential in the vicinity of the initial position of the centroid,  $n_0 = 48$ . Thus, the oscillations found can be referred as to *zero-field* Bloch-like oscillations. To prove this statement, one should bear in mind that at short times the spread is small on the scale of the aperiodic potential [see Fig. 2(b)], so that the latter can be represented by two first terms of its Taylor expansion around the initial position of the centroid. Then, the potential derivative  $d\varepsilon_n/dn$  determines the local field strength which, in the dimensionless units, should be interpreted as the frequency of zero-field Bloch-like oscillations, similarly to the biased Bloch oscillations (see the preceding Section). Applying this reasonings to the site  $n_0 = 48$ , we find that the potential derivative is about  $-0.14$  at this site [see Fig. 1(b)], whose absolute value is indeed fairly close to the frequency of oscillations 0.13 extracted from the centroid dynamics. This is

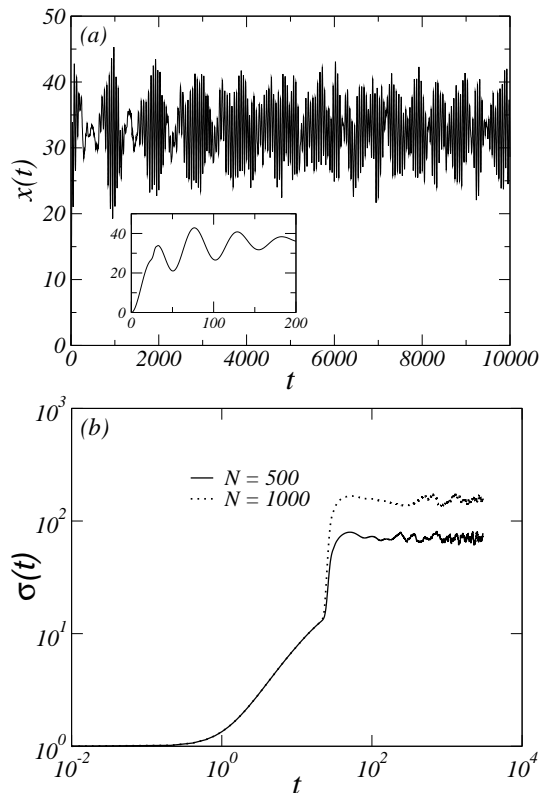


FIG. 2: (a) Time-domain dynamics of the centroid of an unbiased wave packet ( $\sigma = 1$ ,  $n_0 = 48$  at  $t = 0$ ). The inset shows the coherent oscillations at short times. (b) Time-domain dynamics of the wave function spread for two different system sizes.

an unambiguous confirmation of our qualitative picture. It is to be noticed, however, that these arguments fail in the vicinities of potential maxima and minima, where the potential slope is vanishingly small.

As was already mentioned, the zero-field oscillations are not sustained for a long time. When the wave packet spread becomes comparable with the local scale of the aperiodic potential, the nature of the latter, with its wells and barriers, comes into play. This results in losing the phase memory of the wave function. In Fig. 2(b) we depicted the time-domain behavior of the wave packet spread. It displays a ballistic regime within some time interval presented by a linear in log-log scale dependence, followed further by a saturation at some value which, from one hand, depends on the system size, but from the other hand, is considerably smaller than that size. One can also see that the wave packet spread reveals a steep increase at some instant of time which is almost size independent. We relate this features to the tunneling of the wave packet from the potential well, where it was initially located, to the adjacent one. Figure 3 illustrates this tunneling process.

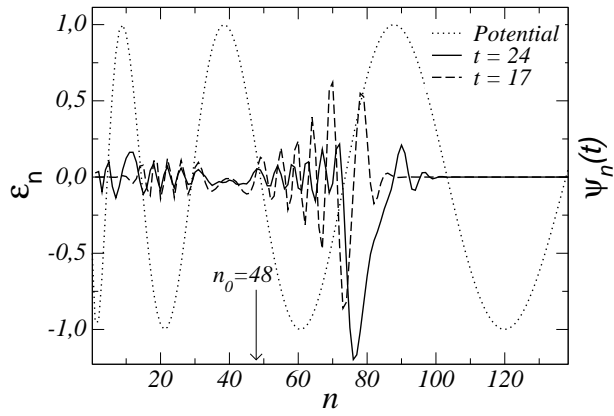


FIG. 3: Wave packet profile  $\Psi_n(t)$  (in arbitrary units) calculated for two moments of time, displaying the tunneling process from the initial potential well. All parameters are the same as in Fig. 2.

### B. Bias effects

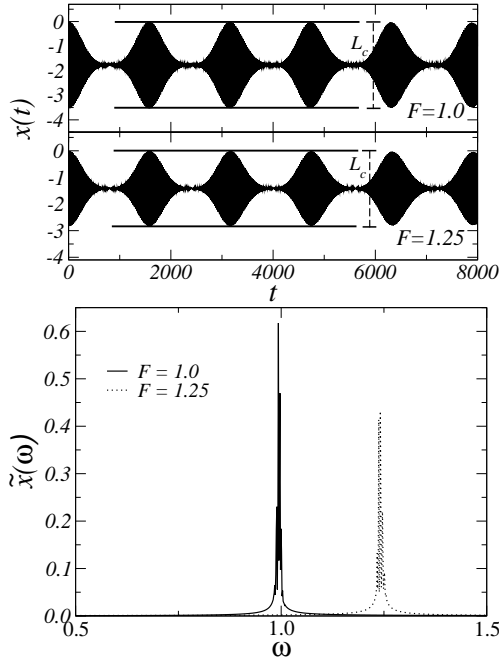


FIG. 4: (a) Time-domain dynamics of the centroid of a biased wave packet ( $n_0 = N/2$  and  $\sigma = 1$  at  $t = 0$ ) for two values of the applied electric field  $F = 1$  and  $1.25$ . (b) Fourier transform of the centroid.

Once a uniform static electric field is turned on, the wave packet dynamics presents quite distinct features as compared to the unbiased behavior. In Fig. 4(a) we plotted the centroids of wave packets calculated for distinct field strengths for the initial position at the chain center. It should be noticed that now Bloch oscillations remain sustained, i.e., no dephasing is taking place. Second, the oscillation amplitude is proportional to  $1/F$  as pre-

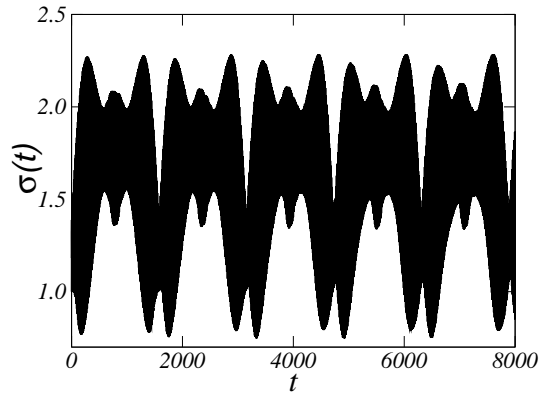


FIG. 5: Time-domain dynamics of the wave function spread of a biased wave packet ( $n_0 = N/2$  and  $\sigma = 1$  at  $t = 0$ ). Notice its localized and breathing nature.

dicted semiclassically. To provide further confirmation of the semiclassical picture, we calculated numerically the Fourier transform of the centroid,  $\tilde{x}(\omega)$ , as shown in Fig. 4(b). Again, the estimated predominant frequency of the Bloch oscillations  $\omega = F$  is corroborated. The localized character of the wave packet is revealed in Fig. 5 where the spread of the wave function is shown; it saturates at a finite value independent of the chain size, displaying however periodic oscillations. The latter characterize the breathing nature of the oscillating wave packet.

As already mentioned, the oscillations are not damped but remain amplitude-modulated. Solid lines in Fig. 4(a) bound the spatial region within which the wave packet oscillates for a long time. The extent of this region  $L_c$  is found to be  $L_c \sim W_c/F$ , where  $W_c$  is independent of the applied field  $F$ . From the data in Fig. 3 we obtain  $W_c \sim 2E_c$ . This value agrees remarkably well with the width of the band of extended states reported in Ref. 22. Thus, we arrive at one of the main conclusions of this work, namely there exist clear signatures of Bloch oscillations of a biased Gaussian wave packet between the two mobility edges.

Some of the above characteristics of the Bloch oscillations can depend on the initial location of wave packets. In particular, at the chain center the underlying aperiodic potential has an almost null derivative. Under this condition, the bias is solely due to the external field. In general, there is a contribution to the external field coming from the aperiodic potential; the total field at position  $n_0$  is given by  $F_{\text{eff}} = d\varepsilon_n/dn + F$ . The local contribution to the applied electric field shall be relevant whenever the potential gradient (in appropriate units) is of the order of the applied field. This is illustrated in Fig. 6(a) with wave packets starting at locations with positive and negative potential gradients. One can see that the oscillation amplitude becomes larger near regions with positive gradients and smaller for negative ones as compared with the results obtained in Fig. 4 for the same applied electric field. Further, the characteristic frequency of these oscillations also exhibits shifts which are of the order of

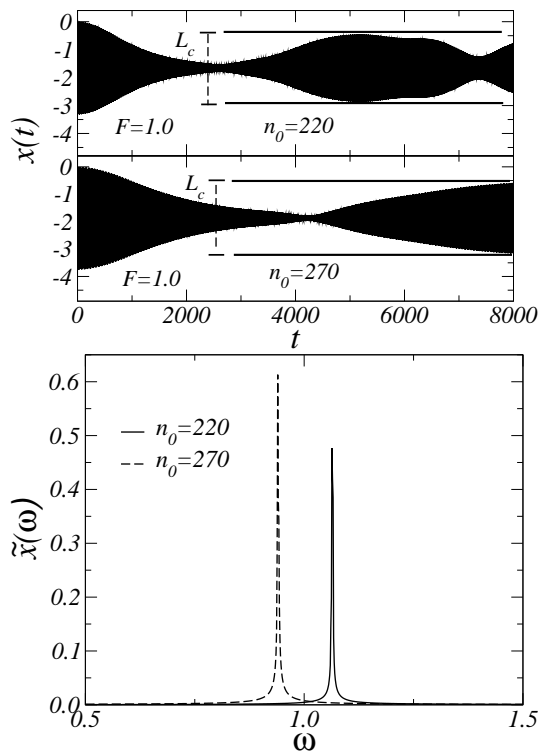


FIG. 6: (a) Time-domain dynamics of the centroid of a biased wave packet ( $\sigma = 1$  at  $t = 0$ ) for  $F = 1$  and two different initial positions. (b) Numerical Fourier transform of the centroid.

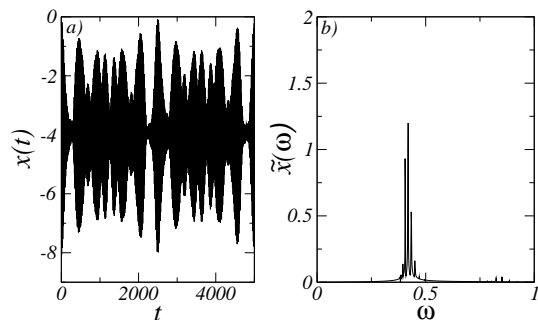


FIG. 7: (a) Time-domain dynamics of the centroid of a biased wave packet ( $n_0 = 48$  and  $\sigma = 1$  at  $t = 0$ ) and  $F = 0.5$ . (b) Numerical Fourier transform of the centroid. The multi-mode structure reveals the spread of the wave function on multiple potential wells.

the local potential gradient [see Fig. 1(b)], as depicted in Fig. 6(b).

As a final remark, the Bloch oscillations shall develop a more complex structure for wave packets initially located near the beginning of the chain, especially at small electric fields for which the amplitude of the oscillations is large enough. Then the wave packet can probe regions with distinct scales of the potential gradient. In Fig. 7 we show a particular case of the dynamics of a wave packet starting at  $n_0 = 48$  under the applied field  $F = 0.5$ . Notice the rich pattern of the centroid oscillations. Its

Fourier transform exhibits multi-mode structure with a series of narrow peaks which are shifted from  $\omega = F$  by quantities that are of the order of the maximum potential gradients at the region covered by the wave packet. The shifts to smaller frequencies can be much easily detected once the initial packet is concentrated at a region of negative potential gradient. However, the corresponding shifts to higher frequency can still be detected too as a series of small peaks.

#### IV. SUMMARY AND CONCLUDING REMARKS

We studied theoretically the single-electron wave packet dynamics within a tight-binding model with an aperiodic slowly varying site potential under the influence of a static uniform electric field. The on-site potential parameters were chosen such that, in the absence of the electric field, the model supports a phase of delocalized states at the center of the band, similarly to high dimensional disordered systems. The electric field promotes a bias which localizes the electron states. The resulting wave packet dynamics reveals Bloch oscillations. However, contrary to what occurs in disordered systems, where scattering on site potential fluctuations gradually degrades the oscillations, these remain sustained with no signature of depletion.

The slowly varying aperiodic nature of the potential results in an additional local bias. Thus, the total bias has contributions of both the aperiodic potential and the one of the applied field. By defining an effective local field, we could show that the amplitude of the oscillations agrees well with the semiclassical prediction and can be used to estimate the width of the band of extended states. The typical frequency of these oscillations can also be understood on the semiclassical grounds. In particular, it is shifted depending on the local potential gradient. In the weak field limit, these oscillations exhibit a multi-mode structure as the wave packet probes a larger region of the aperiodic potential.

Our findings indicate that Bloch oscillations can indeed be observed in superlattices with slowly varying periodicity. The richness of the predicted dynamical behavior can lead to new electro-optical devices, aiming to explore the coherent motion of confined electrons. We hope that the present work will stimulate experimental activities along this direction.

#### Acknowledgments

We are very thankful to H. Yamada for bringing to our attention the problem of aperiodic potentials with mobility edges. Work at Brazil was supported by CNPq and CAPES (Brazilian research agencies) and FAPEAL (Alagoas State agency). Work at Madrid was supported by DGI-MCyT (MAT2003-01533).

- 
- \* On leave from “S.I. Vavilov State Optical Institute”, 199034 Saint-Petersburg, Russia.
- <sup>1</sup> P. W. Anderson, Phys. Rev. **109**, 1492 (1958).
  - <sup>2</sup> N. Mott, Adv. Phys. **16**, 49 (1967).
  - <sup>3</sup> P. A. Lee and T. V. Ramakrishnan, Rev. Mod. Phys. **57**, 287 (1985).
  - <sup>4</sup> B. Kramer and A. MacKinnon, Rep. Prog. Phys. **56**, 1469 (1993).
  - <sup>5</sup> N. Mott and W. D. Twose, Adv. Phys. **10**, 107 (1961).
  - <sup>6</sup> E. Abrahams, P. W. Anderson, D. C. Licciardello, and T. V. Ramakrishnan, Phys. Rev. Lett. **42**, 673 (1979).
  - <sup>7</sup> J. C. Flores, J. Phys.: Condens. Matter **1**, 8471 (1989).
  - <sup>8</sup> D. H. Dunlap, H.-L. Wu, and P. W. Phillips, Phys. Rev. Lett. **65**, 88 (1990).
  - <sup>9</sup> P. W. Phillips and H.-L. Wu, Science **252**, 1805 (1991).
  - <sup>10</sup> A. Sánchez and F. Domínguez-Adame, J. Phys A: Math. Gen. **27**, 3725 (1994); A. Sánchez, E. Maciá, and F. Domínguez-Adame, Phys. Rev. B **49**, 147 (1994).
  - <sup>11</sup> E. Diez, A. Sánchez, F. Domínguez-Adame, Phys. Rev. B **50**, 14359 (1994); F. Domínguez-Adame, E. Diez, and A. Sánchez, Phys. Rev. B **51**, 8115 (1995).
  - <sup>12</sup> V. Bellani, E. Diez, R. Hey, L. Toni, L. Tarricone, G. B. Parravicini, F. Domínguez-Adame, and R. Gómez-Alcalá, Phys. Rev. Lett. **82**, 2159 (1999).
  - <sup>13</sup> F. A. B. F. de Moura and M. L. Lyra, Phys. Rev. Lett. **81**, 3735 (1998); Physica A **266**, 465 (1999).
  - <sup>14</sup> F. M. Izrailev and A. A. Krokhin, Phys. Rev. Lett. **82**, 4062 (1999).
  - <sup>15</sup> U. Kuhl, F. M. Izrailev, A. A. Krokhin, and H.-J. Stöckmann, Appl. Phys. Lett. **77**, 633 (2000).
  - <sup>16</sup> J. C. Cressoni and M. L. Lyra, Physica A **256**, 18 (1998).
  - <sup>17</sup> A. Rodríguez, V. A. Malyshev, and F. Domínguez-Adame, J. Phys. A: Math. Gen. **33**, L161 (2000).
  - <sup>18</sup> A. Rodríguez, V. A. Malyshev, G. Sierra, M. A. Martín-Delgado, J. Rodríguez-Laguna, and F. Domínguez-Adame, Phys. Rev. Lett. **90**, 27404 (2003).
  - <sup>19</sup> D. R. Grempel, S. Fishman, and R. E. Prange, Phys. Rev. Lett. **49**, 833 (1982).
  - <sup>20</sup> M. Griniasty and S. Fishman, Phys. Rev. Lett. **60**, 1334 (1988).
  - <sup>21</sup> D. J. Thouless, Phys. Rev. Lett. **61**, 2141 (1988).
  - <sup>22</sup> S. Das Sarma, S. He, and X. C. Xie, Phys. Rev. Lett. **61**, 2144 (1988); Phys. Rev. B **41**, 5544 (1990).
  - <sup>23</sup> H. Yamada, Phys. Rev. B **69**, 014205 (2004).
  - <sup>24</sup> F. Bloch, Z. Phys. **52**, 555 (1927).
  - <sup>25</sup> G. H. Wannier, Phys. Rev. **100**, 1227 (1955); Phys. Rev. **101**, 1835 (1956); Phys. Rev. **117**, 432 (1960); Rev. Mod. Phys. **34**, 645 (1962).
  - <sup>26</sup> D. H. Dunlap and V. M. Kenkre, Phys. Rev. B **34**, 3625 (1986).
  - <sup>27</sup> K. Leo, P. Hairing, F. Brüggemann, R. Schwedler, and K. Köhler, Solid State Commun. **84**, 943 (1992).
  - <sup>28</sup> K. Leo, Semicond. Sci. Technol. **13**, 249 (1998).
  - <sup>29</sup> V. Agarwal, J. A. Del-Río, G. Malpuech, M. Zanghì, A. Kavokin, D. Conquillat, D. Scabert, M. Vladimirova, and B. Gil, Phys. Rev. Lett. **92**, 097401 (2004).
  - <sup>30</sup> F. Domínguez-Adame, V. A. Malyshev, F. A. B. F. de Moura, and M. L. Lyra, Phys. Rev. Lett. **91**, 197402 (2003).
  - <sup>31</sup> H. N. Nazareno and P. E. de Brito, Phys. Rev. B **60**, 4629 (1999).
  - <sup>32</sup> H. N. Nazareno, C. A. A. da Silva and P. E. de Brito, Superlattices and Microstructures **18**, 297 (1995).
  - <sup>33</sup> N. W. Ashcroft and N. D. Mermin, *Solid State Physics* (Saunders College Publishers, New York, 1976), P. 213.
  - <sup>34</sup> W. H. Press, B. P. Flannery, S. A. Teukolsky, and W. T. Vetterling, *Numerical Recipes: The Art of Scientific Computing* (Cambridge University Press, New York, 1986) pp. 656-663.